ISSN 1946-7664. MCFNS 2017
Vol. 9, Issue 2, pp. 30–33
Mathematical and Computational Forestry & Natural-Resource Sciences

AVAILABLE ONLINE AT HTTP://MCFNS.COM

Submitted: Sep. 18, 2017
Accepted: Sep. 30, 2017
Published: Sep. 30, 2017
Last Correction: Sep. 30, 2017

PHOTOGRAMMETRIC POINT CLOUD TREES

Rong Fang[1], Bogdan Strimbu[1*]

[1] *College of Forestry, Oregon State University, Corvallis, OR, USA*
[*] *corresponding author*

Abstract. This note describes the point clouds representing the stem of three loblolly pines (*Pinus taeda Lindl.*) from west-central Louisiana reconstructed with terrestrial photogrammetry. After capturing the images needed for the 3D rendering, we cut the trees down and measured their diameters at breast height and at every meter along the stem starting at 1 m above the ground. The diameters measured in the field were stored as ASCII files. The reconstructed models reached over 50% of the relative height – the proportion of the stem on which the majority of the merchantable volume is located. For each tree, two files were produced, a point cloud and a mesh data, to represent the 3D stem and some branches. The point cloud was stored in the LAS format and the mesh in the DXF format. Diameter at breast height was marked on all trees by red rings. The files describing the three trees provide a calibrated dataset that can be used for development of taper models, testing and calibration of segmentation algorithms, and identification of products that can be obtained from a stem.

Keywords: structure from motion; loblolly pine; LAS file; DXF file.

1 Introduction

Identifications of the products that can be obtained from each tree requires efficient and accurate stem diameter measurements (Avery and Burkhart 2015, Burkhart and Tomé 2012, Husch et al. 1982). Traditionally, stem measurements on standing trees are time-consuming, expensive, and prone to large errors. In comparison, with conventional measurements (e.g., tree climbing, harvesting), photogrammetric based estimates require less time and involve minimum fieldwork. Instead of measuring the actual stem, the photogrammetric-based approach reconstructs the stem, from images, as a 3D object. Structure from motion (SfM) is a popular method of 3D reconstruction of objects from photos (Dellaert et al. 2000, Forsyth and Ponce 2011, Koenderink and Van Doorn 1991, Weng et al. 1989). SfM builds point clouds from the surfaces of the objects by depicting their geometric characteristics. Some studies have demonstrated that the point clouds derived from SfM are comparable with point clouds generated from laser scanning (Fang and Strimbu 2017, Forsman et al. 2016, Mikita et al. 2016). However, photogrammetry is more affordable than laser scanning (Mancini et al. 2013, Wallace et al. 2016, Westoby et al. 2012), as it involves only minimal investments in equipment and software.

Questions about the ability of using photogrammetric point clouds (henceforth PPC) as a surrogate for stem measurements were addressed by many studies (Fang and Strimbu 2017, Forsman et al. 2016, Mikita et al. 2016). However, there are no PPC known to the authors that are publicly available and can be used for testing algorithms or procedures relevant to this subject.

The objective of this note is to make such a dataset available publicly to any researchers and practitioners, who might be inclined to explore this kind of work. The dataset presented here describes three 3D trees reconstructed from images and associated with them manual stem measurements.

2 Methods

The dataset presented here was developed to demonstrate the applicability and accuracy of the phonogrammically based remote sensing technique for measurement of stem diameters (Fang and Strimbu 2017). It is recognized that the geometric reconstruction of the 3D data from the images introduces bias in the PPC (Daniilidis and Spetsakis 1997, Oliensis 2000, Weng et al. 1989). The bias caused by production of the PPC is minor compared with the bias of diameter measured from PPC (Fang and Strimbu 2017). Therefore, in the respective research

Fang and Strimbu (2017) focused on correcting the bias of the estimated diameters along the stem. From the 18 trees that were used in the study of Fang and Strimbu (2017), we present the three that had the smallest biases.

2.1 Study site and field data collections The study site is located in west central Louisiana, in Vernon parish. The PPC were developed for loblolly pines (*Pinus taeda* Lindl.) positioned in the dominant and codominant crown classes. Field data collection was conducted in February, March, and April, 2014. Before any measurement or photo was recorded the trees were prepared for subsequent data processing, particularly scaling of point clouds. To scale the point clouds two metal bars of 304.8 mm (i.e., 1 foot) were freely hanged on the stem, close to breast height, on opposing sides. The diameter at breast height (DBH) was marked with red paint, which provided additional information for calibration. To identify each tree, on the stem on two opposing sides were written the number of the tree (i.e., id of the tree within the study) and the side of the tree (i.e. 1 or 2). Once preparation was completed, for standing trees, we measured the DBH and captured photographs around each tree. After the photographs were recorded the trees were cut. On the fallen trees, we measured the diameters every meter and at breast height. Diameter measurement were accurate at 1 mm while stem length was measured with 10 mm accuracy. The precision of the measurements were 1 mm for both diameter and length.

To estimate the total height of the trees, the study site was scanned with airborne laser scanners four months earlier than the actual field sampling. The average point density for the LIDAR point cloud is 30 points / m^2. We determine the total heights for the three trees as the largest normalized elevation, which supplied 25.36 m for tree#1, 26.81 m for tree#2, and 18.91 m for tree #2. We compared the LIDAR based values with the fallen trees measurements and we found that they were within 3 cm, for tree #1 and 3 smaller, and for tree#2 larger. Larger height estimated from LIDAR is likely the results of breaking the top part of the tree during the falling process, which justifies the heights based on LIDAR. The corresponding DBH measured in the field are 398.5 mm, 326.0 mm, and 268 mm (Tab. 1).

To reconstruct the trees data we captured red-green-blue (RGB) images of trees with a Nikon D3200 camera equipped with a Nikkor AF-S DX VR 18–55 mm zoom lens (aperture 3.5–5.6). We used the minimum focal length to acquire the images with the largest exposure of the stem of the trees. Multiple images were captured from an approximate circular trajectory surrounding each tree (Fig. 1). Two images were taken at each spot; one was captured with the camera facing directly the tree (i.e., the lens was approximately horizontal), which covered the lower part of the stem, and one was captured with the lens facing the upper part of the stem (i.e., the lens was tilted upwards). Each pair of such images had at least 50% overlap to ensure the successful feature extraction for 3D construction.

Table 1: Diameter along the stem measured in the field for the tree trees

Length on the stem [m]	Diameter [mm] Tree 1	Tree 2	Tree 3
1.0	397	332	280
1.3	399	326	268
2.0	409	320	272
3.0	376	303	262
4.0	382	302	256
5.0	378	288	253
6.0	369	287	237
7.0	363	277	228
8.0	350	269	225

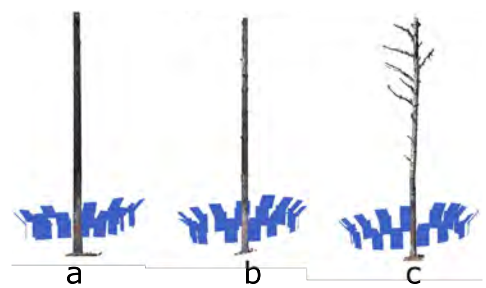

Figure 1: . Position of the cameras to reconstruct the three trees: a. Tree#1, b. Tree#2, c. Tree#3.

2.2 3D model constructions with structure from motion The reconstruction of the trees with SfM was executed in Agisoft PhotoScan version 1.2 (Agisoft LLC 2014). The SfM workflow in Agisoft PhotoScan contains three serial steps: (1) align photos, (2) build dense point cloud, and (3) build mesh. Photo alignment generates the sparse point cloud, which are the features outlining the tree structure. Then, the dense point clouds were generated based on the sparse points to depict the detailed texture of the stem surface. Finally, the mesh model was derived as triangulated irregular network from the dense point clouds.

The accuracy of the 3D models is determined by the quality of the original images and the settings of the parameter defining each step. However, higher accuracy is achieved at the cost of longer computation time. Thus, the selections of the model accuracy rely on the objectives of the study. High resolution and abundance of images are preferred in constructing accurate 3D models (Turner et al. 2014). There are five accuracy options for photo alignment in Agisoft, varying from lowest to highest. The highest accuracy setting allows the program to use the maximum resolution (i.e., in our case: 3872 2592 pixels) to determine the locations of the cameras. For every decreasing level of accuracy, the program down-scales each side of images with half. The images were recorded under the canopy, where GPS signal was weak (i.e., inaccurate positions), which forced their alignment only on the images themselves. To compensate the lack of GPS, we set the accuracy to high, although Liang et al. (2014) demonstrated that low accuracy would be sufficient for accurate measurements. The key point and tie point limits were set to 600,000 and 100,000 respectively. The key points are points extracted from each image, and the tie points are selected from the key points as the most relevant in connecting the images (Ducke et al. 2011). After the images were successfully aligned, Agisoft built the dense point cloud based on the tie points selected during photo alignment. The quality of dense points determines the amount of details identified on the surface of the stem (Ducke et al. 2011). To ensure that the measurements based on PPC are comparable with the field measurements, we set the quality of building dense points to high, with depth filtering disabled. The number of points describing each tree are 2,283,160 for tree #1, 5,148,910 for tree #2, and 1,321,536 for tree #3. After the dense point clouds were created, the mesh was constructed using an arbitrary surface type and the interpolation disabled. Arbitrary surface type is applicable to many types of surfaces, included tree bark. To ensure accurate representation of the stem by the mesh, no interpolations were allowed (Fig.2–4).

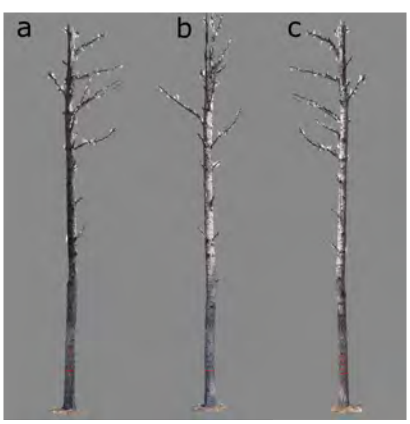

Figure 2: 3D reconstruction of the tree#1, seen from three perspectives (a. south view, b. east view, and c. north view).

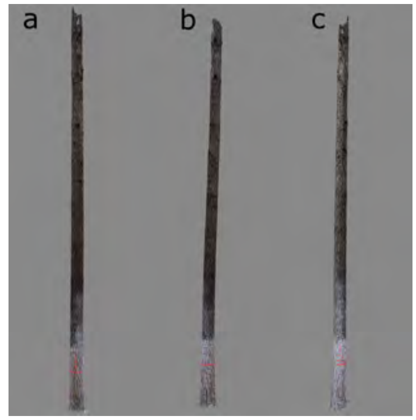

Figure 3: 3D reconstruction of tree#2, seen from three perspectives (a. south view, b. east view, and c. north view).

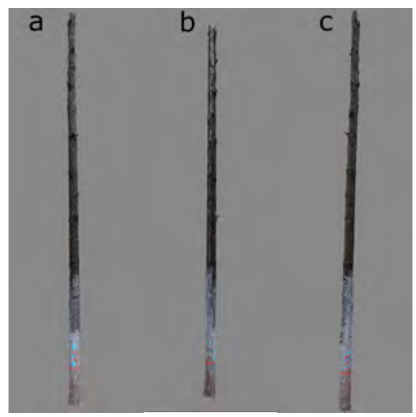

Figure 4: 3D reconstruction of the tree#3, seen from three perspectives (a. south view, b. east view, and c. north view).

The final products (i.e., dense point cloud and mesh) were scaled using the geometric information recorded in the field. Scaling was executed by manually assigning the actual known size to objects identified inside the PPC, such as DBH or metal bars. Scaling based on objects with different orientations are preferred for accurate scaling on all directions. Consequently, the metal bars were used for vertical scaling, while the field marked DBH served for horizontal scaling. Agisoft reported a mean scaling errors of 5 mm on vertical direction and of 4 mm on horizontal directions.

2.3 Access to data and metadata content The data is hosted by the ScholarArchive@OSU, a digital service supported by Oregon State University. The data can be accessed at the persistent URL http://hdl.handle.net/1957/61881. The metadata are located at the same address, and are stored in the file

README_PPC_3Dtrees.txt. The data can be used without restrictions, but acknowledgement of their origin is necessary.

For each of the three trees the following files are available:

- an ASCII file with two fields:
  - field #1, titled "Length_m" contains the height in meters along the stem, and
  - field #2, titled "Diameter_mm", contains the diameter in millimeters at the respective height;
- a LAS file with the colored point clouds, and
- an Autodesk drawing interchange format file (DXF) that stores the mesh model. The top number on the tree mesh data represent the tree id, and the bottom number on the tree mesh data represents the north side (i.e., 1) and the south side (i.e., 2).

The files are identified using the following convention: Tree#_field.txt, for the field measurements, Tree#_PPC.las for the photogrammetric point cloud, and Tree#_mesh.dxf for the mesh model of the tree. The "#" represents the tree number: 1, 2, or 3.

References

Agisoft LLC. 2014. Agisoft Photoscan. Agisoft, St. Petersburg, Russia.

Avery, T.E. and Burkhart, H.E. 2015. Forest measurements. Waveland Press.

Burkhart, H.E. and Tomé, M. 2012. Modeling forest trees and stands. Springer Science & Business Media.

Daniilidis, K., and Spetsakis, M.E. 1996. Understanding noise sensitivity in structure from motion. In Visual Navigation. Edited by Y. Aloimonos. Lawrence Erlbaum Associates, Hillsdale NJ USA. Pp. 61–88.

Dellaert, F., Seitz, S.M., Thorpe, C.E. and Thrun, S. 2000. Structure from motion without correspondence. IEEE Conference on Computer Vision and Pattern Recognition, Proceedings. Pp. 557–564.

Ducke, B., Score, D. and Reeves, J. 2011. Multiview 3D reconstruction of the archaeological site at Weymouth from image series. *Computers & Graphics*, **35**, 375–382.

Fang, R. and Strimbu, B. 2017. Stem Measurements and Taper Modeling Using Photogrammetric Point Clouds. *Remote Sensing*, **9**, 21.

Forsman, M., Börlin, N. and Holmgren, J. 2016. Estimation of Tree Stem Attributes Using Terrestrial Photogrammetry with a Camera Rig. *Forests*, **7**, 61.

Forsyth, D. and Ponce, J. 2011. Computer vision: a modern approach. Upper Saddle River, NJ; London: Prentice Hall.

Husch, B., Miller, C.I. and Beers, T.W. 1982. Forest mensuration. John Wiley & Sons, Inc.

Koenderink, J.J. and Van Doorn, A.J. 1991. Affine structure from motion. *Journal of the Optical Society of America A*, **8**, 377–385.

Liang, X.L., Jaakkola, A., Wang, Y.S., Hyyppa, J., Honkavaara, E., Liu, J.B. *et al.* 2014. The Use of a Hand-Held Camera for Individual Tree 3D Mapping in Forest Sample Plots. *Remote Sensing*, **6**, 6587-6603.

Mancini, F., Dubbini, M., Gattelli, M., Stecchi, F., Fabbri, S. and Gabbianelli, G. 2013. Using unmanned aerial vehicles (UAV) for high-resolution reconstruction of topography: The structure from motion approach on coastal environments. *Remote Sensing*, **5**, 6880-6898.

Mikita, T., Janata, P. and Surový, P. 2016. Forest Stand Inventory Based on Combined Aerial and Terrestrial Close-Range Photogrammetry. *Forests*, **7**, 165.

Oliensis, J. 2000. A Critique of Structure-from-Motion Algorithms. *Computer Vision and Image Understanding*, **80**, 172-214.

Turner, D., Lucieer, A. and Wallace, L. 2014. Direct georeferencing of ultrahigh-resolution UAV imagery. *IEEE Transactions on Geoscience and Remote Sensing*, **52**, 2738-2745.

Wallace, L., Lucieer, A., Malenovský, Z., Turner, D. and Vopěnka, P. 2016. Assessment of Forest Structure Using Two UAV Techniques: A Comparison of Airborne Laser Scanning and Structure from Motion (SfM) Point Clouds. *Forests*, **7**, 62.

Weng, J., Huang, T.S. and Ahuja, N. 1989. Motion and structure from two perspective views: Algorithms, error analysis, and error estimation. *IEEE Transactions on Pattern Analysis and Machine Intelligence*, **11**, 451-476.

Westoby, M., Brasington, J., Glasser, N., Hambrey, M. and Reynolds, J. 2012. 'Structure-from-Motion'photogrammetry: A low-cost, effective tool for geoscience applications. *Geomorphology*, **179**, 300-314.